Wound healing defect of *Vav3*$^{-/-}$ mice due to impaired β_2-integrin–dependent macrophage phagocytosis of apoptotic neutrophils

*Anca Sindrilaru,[1] *Thorsten Peters,[1] Jürgen Schymeinsky,[2] Tsvetelina Oreshkova,[1] Honglin Wang,[1] Anne Gompf,[3] Francesca Mannella,[4] Meinhard Wlaschek,[1] Cord Sunderkötter,[5] Karl Lenhard Rudolph,[3] Barbara Walzog,[2] Xosé R. Bustelo,[6] Klaus D. Fischer,[4,7] and Karin Scharffetter-Kochanek[1]

[1]Department of Dermatology and Allergic Diseases, University of Ulm, Ulm, Germany; [2]Walter-Brendel-Centre for Experimental Medicine, Ludwig Maximilians University, Munich, Germany; [3]Institute of Molecular Medicine and Max-Planck-Research Group on Stem Cell Aging and [4]Department of Physiologic Chemistry, University of Ulm, Ulm, Germany; [5]Department of Dermatology and Venerology, University of Münster, Münster, Germany; [6]Centro de Investigación del Cáncer, CSIC–University of Salamanca, Salamanca, Spain; and [7]Institute of Biochemistry and Cell Biology, University of Magdeburg, Magdeburg, Germany

Vav proteins are guanine-nucleotide exchange factors implicated in leukocyte functions by relaying signals from immune response receptors and integrins to Rho-GTPases. We here provide first evidence for a role of Vav3 for β_2-integrins–mediated macrophage functions during wound healing. *Vav3*$^{-/-}$ and *Vav1*$^{-/-}$/*Vav3*$^{-/-}$ mice revealed significantly delayed healing of full-thickness excisional wounds. Furthermore, *Vav3*$^{-/-}$ bone marrow chimeras showed an identical healing defect, suggesting that Vav3 deficiency in leukocytes, but not in other cells, is causal for the impaired wound healing. Vav3 was required for the phagocytotic cup formation preceding macrophage phagocytosis of apoptotic neutrophils. Immunoprecipitation and confocal microscopy revealed Vav3 activation and colocalization with β_2-integrins at the macrophage membrane upon adhesion to ICAM-1. Moreover, local injection of *Vav3*$^{-/-}$ *or* β_2-integrin(*CD18*)$^{-/-}$ macrophages into wound margins failed to restore the healing defect of *Vav3*$^{-/-}$ mice, suggesting Vav3 to control the β_2-integrin–dependent formation of a functional phagocytic synapse. Impaired phagocytosis of apoptotic neutrophils by *Vav3*$^{-/-}$ macrophages was causal for their reduced release of active transforming growth factor (TGF)-β_1, for decreased myofibroblasts differentiation and myofibroblast-driven wound contraction. TGF-β_1 deficiency in *Vav3*$^{-/-}$ macrophages was causally responsible for the healing defect, as local injection of either Vav3-competent macrophages or recombinant TGF-β_1 into wounds of *Vav3*$^{-/-}$ mice fully rescued the delayed wound healing. (Blood. 2009;113:5266-5276)

Introduction

Normal tissue repair follows a sequence of events involving clotting, inflammation, granulation tissue formation and re-epithelialization.[1,2] Within few hours after injury, first polymorphonuclear neutrophils (PMN) and later macrophages (Mϕ) invade the wound tissue to combat contaminating organisms by producing proteases and reactive oxygen species (ROS).

By phagocytosing apoptotic PMN before these undergo secondary necrosis, Mϕ terminate the inflammatory phase and prevent spillage of toxic proteases and ROS that might amplify tissue injury.[3] After engulfment of PMN, Mϕ release transforming growth factor (TGF)–β_1 at the wound site,[3,4] which initiates myofibroblast differentiation, wound contraction, and neo-angiogenesis.[4,5]

A large number of leukocyte and endothelial adhesion molecules are required to coordinately regulate the influx and intimate cell-to-cell interactions of distinct leukocyte subpopulations at wound sites.[4,6] The β_2-integrins CD11a/CD18 (LFA-1), CD11b/CD18 (Mac-1), CD11c/CD18 (gp 150,95), and CD11d/CD18 are constitutively expressed on the surface of leukocytes; these heterodimers consist of a common β_2 subunit (CD18) and a variable α subunit (CD11a, CD11b, CD11c, CD11d).[7] β_2-integrins are responsible for PMN recruitment[4,8-12] and for the recruitment of Mϕ subsets[13] in different mouse models of inflammation. In addition, CD18 is crucial for the formation of the phagocytic synapse between Mϕ and apoptotic PMN[14] that initiates TGF-β_1 release and is essential for myofibroblasts differentiation[4] and vessel formation.[5] The importance of β_2-integrins is emphasized in leukocyte adhesion deficiency (LAD1) patients suffering from severe wound healing disturbances and bacterial infections due to decreased β_2-integrin expression and/or function.[15,16] Also *CD18*$^{-/-}$ mice share the essential characteristics of LAD1 patients.[4,10] Thus, β_2-integrins are critical mediators of PMN and Mϕ functions in innate immunity and tissue repair. However, apart from a few downstream target proteins of β_2-integrin signaling such as the nonreceptor tyrosine kinase Syk activated by adaptors bearing immunoreceptor tyrosine based activation motifs (ITAMs),[17,18] little is known on the CD18 downstream signaling in phagocytes.

The guanine-nucleotide exchange factors Vav couple to diverse signaling receptors and, due to their exchange activity and adaptor domains, are ideally suited to transduce signals to RhoGTPases and the actin cytoskeleton.[19-21] Targeted disruption of *Vav1* results in severe impairment of T lymphocyte function in response to antigen receptor stimulation[19,20] with defective TCR capping and actin patch formation.[21,22] Various *Vav* double-knockout mice reveal distinctive B- and T-cell phenotypes,[23-25] and in case of *Vav* triple

Submitted July 10, 2008; accepted December 22, 2008. Prepublished online as *Blood* First Edition paper, January 15, 2009; DOI 10.1182/blood-2008-07-166702.

*A.S. and T.P. contributed equally to this work.

An Inside *Blood* analysis of this article appears at the front of this issue.

The online version of this article contains a data supplement.

The publication costs of this article were defrayed in part by page charge payment. Therefore, and solely to indicate this fact, this article is hereby marked "advertisement" in accordance with 18 USC section 1734.

knockouts, the function of B and T cells is severely compromised.[25] Mainly in vitro evidence exists for FcγR, β_1, β_2 and β_3-integrin–dependent roles for Vav proteins in T cells,[26] platelets,[27] neutrophils,[28-30] and Mϕ.[31,32]

To dissect carefully the in vivo role of Vav proteins for β_2-integrin–dependent PMN and Mϕ functions in cutaneous wound healing, we here used *Vav1*$^{-/-}$, *Vav3*$^{-/-}$, and *Vav1*$^{-/-}$/*Vav3*$^{-/-}$ mice. We identify Vav3 as a critical downstream target in the CD18-dependent formation of the phagocytic synapse between Mϕ and PMN required for tissue repair.

Methods

Mice

Vav1$^{-/-}$, *Vav2*$^{-/-}$, *Vav3*$^{-/-}$, *Vav1*$^{-/-}$/*Vav3*$^{-/-}$, *Vav2*$^{-/-}$/*Vav3*$^{-/-}$, and WT littermates were previously described.[24,33] Wound-healing experiments were performed with male cohorts between 8 and 12 weeks of age. All experiments were carried out in compliance with the German Law for Welfare of Laboratory Animals and were approved by the Institutional Review Board of the University of Ulm.

Generation of bone marrow chimeras

Bone marrow chimeras were generated by intravenous injection of whole bone marrow cells from WT or *Vav3*$^{-/-}$ mice on C57BL/6 (B6) background carrying the Ly5.2/CD45.2 allele, into lethally irradiated congenic recipients bearing the Ly5.1/CD45.1 allele on B6 background (The Jackson Laboratory, Bar Harbor, ME). Complete repopulation with either *Vav3*$^{-/-}$ or WT leukocyte compartment was confirmed by flow cytometry and immunoblotting (Figure S1A,B, available on the *Blood* website; see the Supplemental Materials link at the top of the online article).

Wound-healing model

Wound-healing experiments were performed as described.[4] Briefly, full-thickness (including the *panniculus carnosus*) excisional wounds were produced under anesthesia with 6-mm round knives (Stiefel, Offenbach, Germany) on both sides of the shaved backs of *Vav1*$^{-/-}$, *Vav2*$^{-/-}$, *Vav3*$^{-/-}$, *Vav1*$^{-/-}$/*Vav3*$^{-/-}$, *Vav2*$^{-/-}$/*Vav3*$^{-/-}$, and WT mice, and of WT or *Vav3*$^{-/-}$ chimeras. Four wounds per mouse were induced. At indicated time points, each wound was digitally photographed, and wound areas were quantified using Adobe Photoshop software version 7.0.1 (Adobe Systems, San Jose, CA). Wound sizes at any time point were expressed as percentage of initial (day 0) wound area. For early time point analyses, wounds including adjacent margins were snap-frozen and stored at −80°C.

Immunofluorescence staining, Western blot analysis, and generation of murine bone marrow-derived Mϕ and apoptotic PMN

Details of immunofluorescence staining, Western blot analysis, and generation of murine bone marrow-derived Mϕ and apoptotic PMN are contained in Document S1.

In vitro adhesion and phagocytosis assays

WT or *Vav3*$^{-/-}$ mature Mϕ were plated to adhere onto 24-well cell culture plates (Nunc/Thermo Fisher Scientific, Langenselbold, Germany) before addition of CMRA-labeled apoptotic PMN from indicated genotypes at Mϕ:PMN ratio of 1:10. After 15 minutes of coculture for adhesion and 45 minutes for phagocytosis, nonadherent/ingested PMN were removed with cold phosphate-buffered saline (PBS). Adherent cells were collected by scraping and stained for the Mϕ marker F4/80. CMRA$^+$F4/80$^+$ double positive complexes either of Mϕ adherent to PMN or Mϕ phagocytosing PMN were quantified by flow cytometry as previously described.[4]

Macrophage adhesion assay

Ninety-six-well cell culture plates (Nunc) were coated with 20 μg/mL fibronectin (BD Biosciences, Heidelberg, Germany), 20 μg/mL rmICAM-1 or with 20 μg/mL vitronectin (R&D Systems, Wiesbaden, Germany) overnight at 4°C. Bovine serum albumin (BSA; 0.1%)–coated wells served as controls for unspecific adhesion. BSA covered the plastic, reported to bind β_2-integrins, and thus abolished β_2-integrin–mediated adhesion. WT or *Vav3*$^{-/-}$ 5-chloromethylfluorescein diacetate (CMFDA)–labeled Mϕ preactivated with 10 ng/mL TNFα (PeproTech, Hamburg, Germany) were seeded onto the coated plates at 5×10^4/well, shortly placed on ice to synchronize adhesion and incubated to adhere at 37°C for 15 minutes. Nonadherent cells were rigorously washed with PBS. Adhesion was assessed as percentage of fluorescence intensity related to total input macrophages (100%) measured at 485 nm with a Twinkle LB970 Fluorometer (Berthold Technologies, Bad Wildbad, Germany).

Oxidative burst

WT and *Vav3*$^{-/-}$ Mϕ loaded with the ROS-sensitive fluorescence quenched substrate 5-(and 6)-carboxy-2′,7′-dichlorodihydrofluorescein diacetate (Invitrogen, Karlsruhe, Germany) were incubated with apoptotic PMN at 1:10 ratio for 180 minutes at 37°C. The increase in green fluorescence intensity reflecting oxidative burst was measured by fluorometry.

Immunoprecipitation

To study Vav3 activation, Mϕ lysates were immunoprecipitated with anti-Vav3 pAb (Millipore, Billerica, MA), followed by Western blotting using anti-Phosphotyrosine mAb (4G10;, Millipore). A detailed description is included in Document S1.

Rescue and transfer experiments

Recombinant human (rh) TGF-β_1 (R&D Systems) was subcutaneously injected at physiologic concentrations of 0.45 μg/wound into wound margins at days 1, 3, 5 and 7 after wounding as published.[4] Mice treated with 0.9% saline served as mock controls. For transfer experiments, 10^6 WT, *Vav3*$^{-/-}$ or *CD18*$^{-/-}$ Mϕ/wound were injected at 4 sites into the wound margins of WT or *Vav3*$^{-/-}$ mice. Control wounds were injected with PBS.

Cytokine enzyme-linked immunosorbent assay ELISA

Details of cytokine enzyme-linked immunosorbent assay (ELISA) appear in Document S1.

Binding of soluble ICAM-1

Bone marrow-derived WT, *Vav3*$^{-/-}$ and *CD18*$^{-/-}$ unstimulated (resting) or stimulated (with 100 nm fMLP, 100 nm LTB4; Sigma-Aldrich) or 50 ng/mL TNFα (eBioscience, Frankfurt, Germany) Mϕ were incubated with 5 μg rmICAM-1 fused to the Fc region of human IgG (ICAM-1/Fc; R&D Systems) in 100 μL binding buffer (PBS, 2 mM MgCl2, 1 mM CaCl2, 1 mM D-Glucose and 0.1% BSA) at 37°C for 10 minutes with continuous agitation. Mϕ incubated with human IgG served as controls. Mϕ were immediately fixed on ice in 3.7% paraformaldehyde, washed in PBS and labeled with FITC-conjugated F(ab′) anti–human IgG to detect bound ICAM-1 on Mϕ by flow cytometry. Bound ICAM-1/Fc was assessed as ratio between the mean fluorescence intensities of Mϕ incubated with ICAM-1/Fc and Mϕ incubated with human IgG for each stimulation.

Image acquisition and analysis

Wounds were photographed using a Sony Super SteadyShot DSC-H5 digital camera (Sony Germany, Berlin, Germany). Histology samples were visualized using a Zeiss Axiophot microscope with Plan-NEOFLUAR 20×/0.75 (∞/0.17) objective and images were captured using AxioCam MRc camera and AxioVision Version 4.7 imaging software (all Carl Zeiss, Jena, Germany). Confocal microscopy was performed using LSM 410/Axiovert 135M microscope (Zeiss) with Leica TCS SP% 63×/1.2 oil objective (Leica Microsystems, Wetzlar, Germany). Images were imported

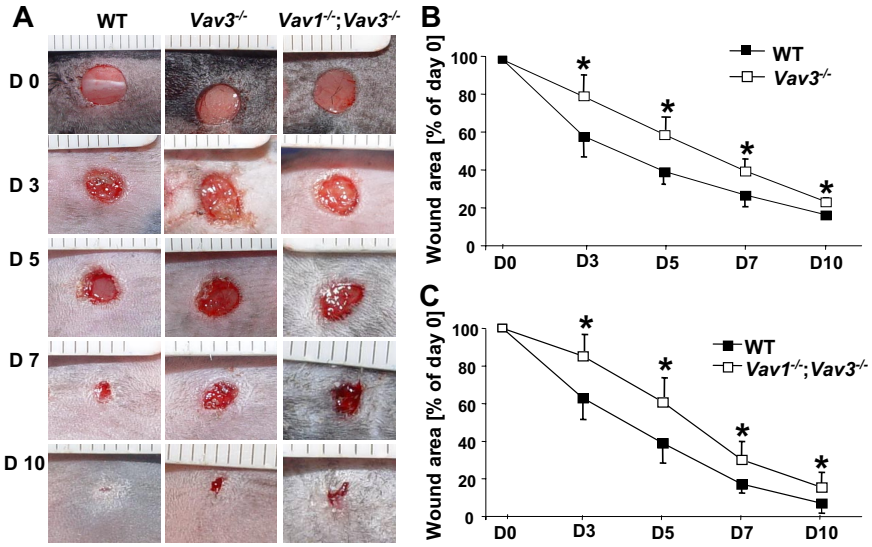

Figure 1. Wound closure of full-thickness wounds is delayed in *Vav3*$^{-/-}$ and *Vav1*$^{-/-}$/*Vav3*$^{-/-}$ mice. (A) Representative macroscopic aspects of wounds from *Vav3*$^{-/-}$, *Vav1*$^{-/-}$/*Vav3*$^{-/-}$ and WT mice at different healing stages. (B,C) Statistical analysis of 24 wound areas quantified at days 0, 3, 5, 7 and 10 after wounding expressed as percentage of the initial (day 0) wound size for WT, *Vav3*$^{-/-}$ and *Vav1*$^{-/-}$/*Vav3*$^{-/-}$ mice. Results given as mean ± SD (n = 6) reflect 1 of 3 independent experiments. *$P < .05$ by Mann-Whitney test.

into and processed using Adobe Photoshop Version 7.0.1 software (Adobe Systems, San Jose, CA).

Statistical analysis

Quantitative data are presented as mean values plus or minus standard deviation (SD). Statistical significance was determined by the 2-tailed Student *t* test, or the Mann-Whitney U test in cases of a non-Gaussian distribution. A *P* value less than .05 was considered statistically significant.

Results

Vav3$^{-/-}$ mice display delayed wound healing with diminished numbers of Mϕ and normal PMN recruitment at the wound site

Full-thickness wounds were produced on *Vav1*$^{-/-}$, *Vav2*$^{-/-}$, *Vav3*$^{-/-}$ mice, intercrosses thereof, and WT controls. Wound sizes were monitored as described.[4] Wound closure of *Vav3*$^{-/-}$ mice was significantly delayed between days 3 and 10 after wounding compared with WT mice (Figure 1A,B). No delay in wound closure was observed in *Vav1*$^{-/-}$ and *Vav2*$^{-/-}$ mice, whereas their intercrosses with *Vav3*$^{-/-}$ mice (*Vav1*$^{-/-}$/*Vav3*$^{-/-}$ and *Vav2*$^{-/-}$/*Vav3*$^{-/-}$) did not aggravate the wound closure deficiency of *Vav3*$^{-/-}$ mice, suggesting that neither Vav1 nor Vav2 deficiency contributed to the delayed wound healing of *Vav3*$^{-/-}$ mice (Figure 1C and data not shown). Therefore, we concentrated on *Vav3*$^{-/-}$ and for control purposes in selected experiments also on *Vav1*$^{-/-}$/*Vav3*$^{-/-}$ mice.

Immunostaining for GR-1 revealed virtually no differences in PMN numbers at wound sites of *Vav3*$^{-/-}$ and *Vav1*$^{-/-}$/*Vav3*$^{-/-}$ compared with WT mice at 24 hours after wounding (Figure 2A). Also at earlier (1 hour, 6 hours) and later (72 hours) time points, no obvious differences in PMN recruitment were observed for the studied genotypes (data not shown). By contrast, immunostaining of 72-hour wounds revealed a significant reduction in recruitment of F4/80$^+$ Mϕ to wound sites of *Vav3*$^{-/-}$ and *Vav1*$^{-/-}$/*Vav3*$^{-/-}$ compared with WT mice (Figure 2A). These data were confirmed by fluorescence-activated cell sorting (FACS) quantification of GR-1$^+$ PMN enzymatically isolated from wound tissue 24 hours after wounding (Figure 2B) and of F4/80$^+$ Mϕ isolated 3 days after wounding (Figure 2C). The expression levels of apoptosis markers such as active caspase-3 and PARP-1 were identical in wounds of WT and *Vav3*$^{-/-}$ mice at different time points (data not shown), suggesting that enhanced apoptosis was not responsible for the reduced Mϕ numbers at *Vav3*$^{-/-}$ wound sites.

Wounds of *Vav3*$^{-/-}$ mice reveal reduced numbers of myofibroblasts and blood vessels

Differences in wound size between WT and *Vav3*$^{-/-}$ mice were most significant between days 3 and 7 after wounding. While at day 3 the early inflammatory phase prevails, we have focused on days 5 and 7, when mainly myofibroblast-dependent wound contraction[34] and neo-angiogenesis occur, and studied the expression of myofibroblasts and endothelial cell markers in granulation tissues by histology and Western blotting. In 5- and 7-day-old wounds, the myofibroblast-specific α smooth muscle actin (αSMA) was abundantly present at wound edges and below the hyperproliferative epidermis of WT wounds. In contrast, only faint αSMA staining was detected in the correspondent areas of 5- and 7-day-old *Vav3*$^{-/-}$ wounds (Figure 2D). Densitometric assessment of Western blots revealed lower expression of αSMA and another myofibroblast marker, TGFβ-RII, in wounds of *Vav3*$^{-/-}$ mice compared with WT mice (Figure 2E,F). Vimentin served to equilibrate loading for similar numbers of fibroblastic cells. These results suggested that lower numbers of myofibroblasts resided in wound beds of *Vav3*$^{-/-}$ mice compared with WT mice.

Apart from myofibroblast-driven wound contraction, neo-angiogenesis plays an important role in tissue repair. Notably, immunostaining for platelet/endothelial cell adhesion molecule 1 (PECAM-1) revealed high numbers of vessels in 5 and 7 days WT wounds, whereas significantly fewer PECAM-1$^+$ vessels were found in *Vav3*$^{-/-}$ wounds (Figure 2D). This was confirmed by Western blotting using wound lysates of *Vav3*$^{-/-}$ and WT mice (Figure 2E,F), suggesting that neo-angiogenesis is reduced and delayed in *Vav3*$^{-/-}$ mice. αSMA, TGFβ-RII, and PECAM-1 in nonwounded normal skin were expressed at identical low levels in the studied *Vav3*$^{-/-}$ and WT mice, excluding the possibility that these molecules are globally down-regulated in *Vav3*$^{-/-}$ mice.

Local injection of TGF-β_1 rescues myofibroblast-driven wound contraction and neo-angiogenesis, but not defective Mϕ recruitment in *Vav3*$^{-/-}$ mice

TGF-β_1 is the pivotal growth factor promoting myofibroblast differentiation[35] and neo-angiogenesis during wound healing.[5]

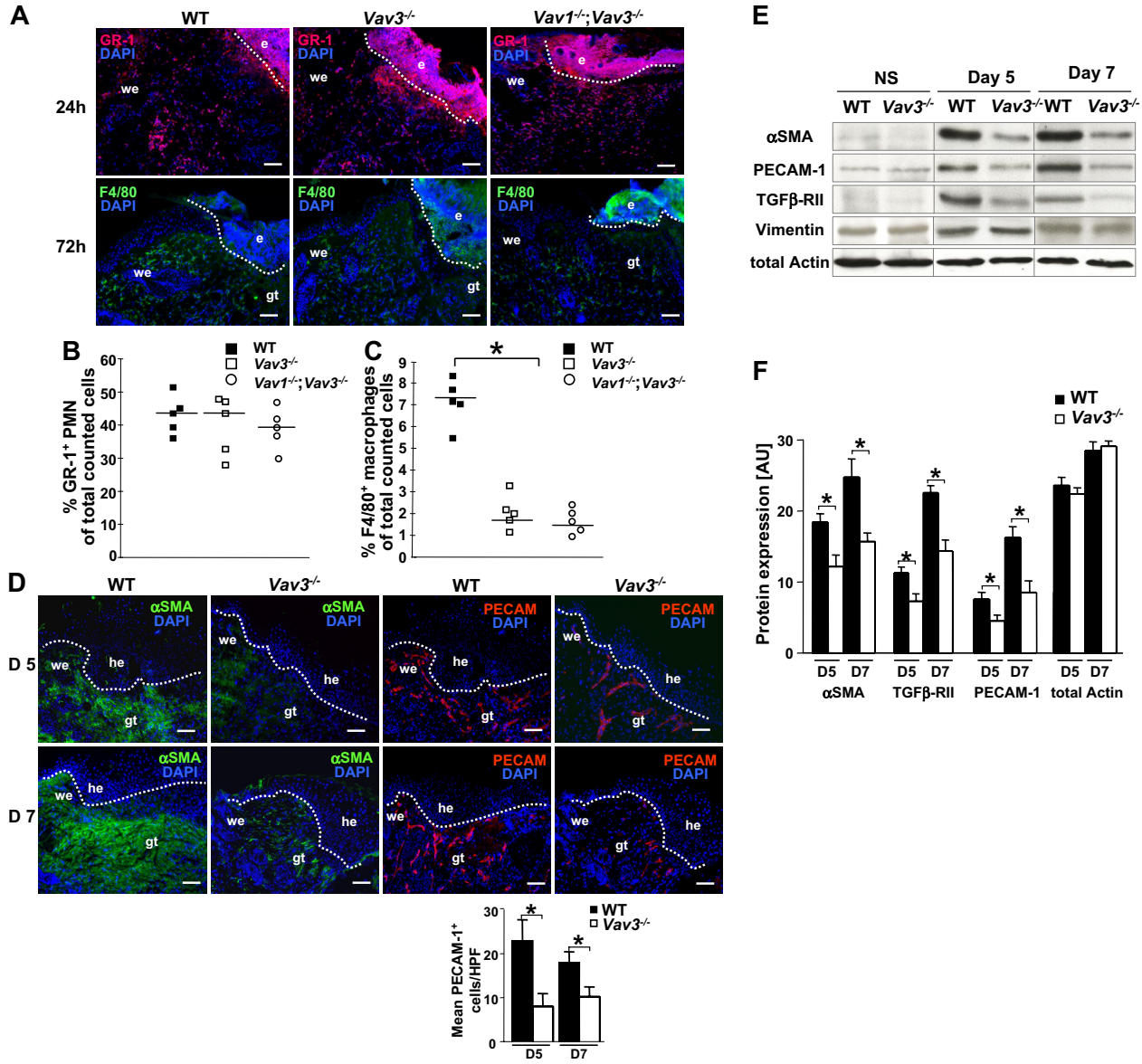

Figure 2. Impaired recruitment of Mϕ, but not of PMN, and reduced numbers of myofibroblasts and blood vessels at the wound sites of *Vav3*$^{-/-}$ mice. (A) GR-1$^+$ PMN (red; top panel) and F4/80$^+$ Mϕ (green; bottom panel) recruitment to wound sites assessed by immunostaining of cryosections from *Vav3*$^{-/-}$, *Vav1*$^{-/-}$/*Vav3*$^{-/-}$ and WT mice. Quantification of GR-1$^+$ PMN recruitment at 24 hours after wounding (B) and F4/80$^+$ Mϕ recruitment at 72 hours after wounding (C) by FACS analysis of wound cells isolated by enzymatic disruption from wound tissue. Results given as scatter plots. Bars indicate the median (n = 5). *$P < .05$ by Student *t* test. (D) Granulation tissue formation in 5 and 7 days old WT and *Vav3*$^{-/-}$ wounds assessed by immunostaining with myofibroblasts-specific αSMA (green) and endothelial cell–specific PECAM-1 (red). Cell nuclei are counterstained with DAPI (blue). Original magnification ×20, scale bar indicates 200μm; e, eschar, he, hyperproliferative epidermis; we, wound edge, gt, granulation tissue. Quantification of PECAM-1$^+$ cells in 10 high-power fields (HPFs) of 5- and 7-day-old wounds of 4 *Vav3*$^{-/-}$ and WT mice. Data are given as mean ± SD numbers of PECAM-1$^+$ cells counted per HPF. *$P < .05$ by Student *t* test. (E) Western blot analysis of snap-frozen nonwounded normal skin (NS) and of wound tissue at days 5 and 7 equilibrated to total actin and vimentin levels to measure expression of αSMA, TGFβ-RII and PECAM-1. αSMA, TGFβ-RII, PECAM-1, actin, and vimentin are expressed at identical levels in WT and Vav3$^{-/-}$ nonwounded skin, excluding that these molecules are globally down-regulated in *Vav3*$^{-/-}$ mice. (F) Semiquantitative balance analysis of immunoblots performed by densitometry of digitized Western blots. Data are given as mean ± SD. *$P < .05$ by Student *t* test.

Rough assessment of TGF-β_1 expression by immunohistology revealed in all genotypes (WT, *Vav3*$^{-/-}$, *Vav1*$^{-/-}$/*Vav3*$^{-/-}$) a strong TGF-β_1 staining in the epidermis and hair follicles, identified by epidermis-specific K14 staining (Figure 3A). There was, however, clearly reduced staining in the dermal wound margins and granulation tissue at days 5 and 7 after wounding of *Vav3*$^{-/-}$ and *Vav1*$^{-/-}$/*Vav3*$^{-/-}$ mice compared with WT mice (Figure 3A and data not shown). To substantiate these findings, total and active TGF-β_1 concentrations were quantified by specific ELISA. Although no significant differences in total TGF-β_1 concentrations were found between WT, *Vav3*$^{-/-}$ and *Vav1*$^{-/-}$/*Vav3*$^{-/-}$ wounds, active TGF-β_1 concentrations were significantly reduced in 5-day-old wound lysates from *Vav3*$^{-/-}$ and *Vav1*$^{-/-}$/*Vav3*$^{-/-}$ mice (Figure 3B). Moreover, upon phagocytosis of apoptotic PMN, *Vav3*$^{-/-}$ Mϕ revealed a significantly decreased oxidative burst compared with WT Mϕ (Figure 3C). As ROS have been shown to convert latent TGF-β_1 to active TGF-β_1,[36] the reduced ROS formation in *Vav3*$^{-/-}$ Mϕ may contribute to the reduced activation of TGF-β_1 in *Vav3*$^{-/-}$ and *Vav1*$^{-/-}$/*Vav3*$^{-/-}$ wound lysates compared with WT wounds. These results provide circumstantial evidence that reduced active TGF-β_1 at wound sites accounts for decreased numbers of αSMA$^+$ myofibroblasts, reduced wound contraction and diminished neovascularization of the restoration tissue in *Vav3*$^{-/-}$ mice.

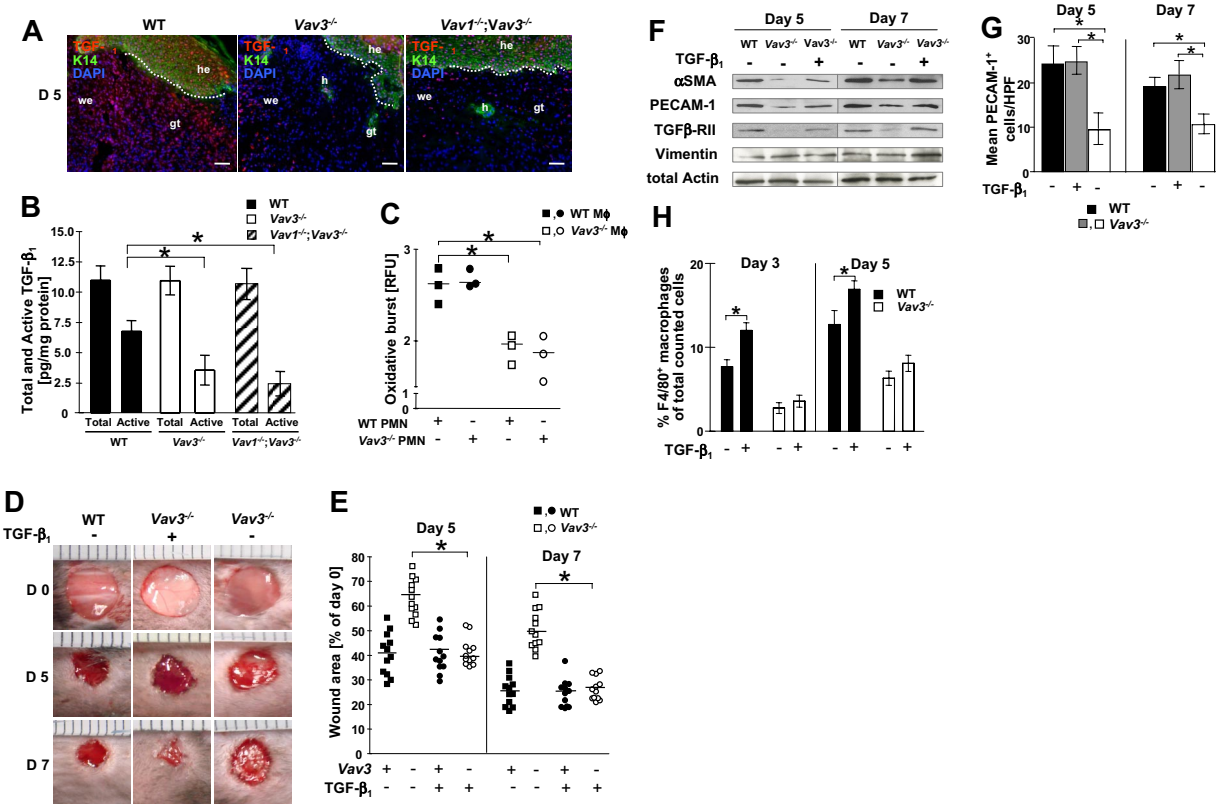

Figure 3. Reduced release of active TGF-β_1 in the wound margins is causal for the wound healing defect of *Vav3*$^{-/-}$ and *Vav1*$^{-/-}$/*Vav3*$^{-/-}$ mice. (A) Immunostaining of 5-day-old wounds from *Vav3*$^{-/-}$, *Vav1*$^{-/-}$/*Vav3*$^{-/-}$ and WT mice showing TGF-β_1 (red) localization throughout the K14$^+$ epidermis (green) and the wound tissue. Blue staining indicates nuclear staining with DAPI. Original magnification ×20, scale bar indicates 200μm; he, hyperproliferative epidermis; we, wound edge, gt, granulation tissue, h, hair follicle. (B) Quantitative evaluation of total and active TGF-β_1 release from 5 days old *Vav3*$^{-/-}$, *Vav1*$^{-/-}$/*Vav3*$^{-/-}$ and WT wound lysates by specific ELISA. Results representative of 2 independent experiments are expressed as mean ± SD (n = 4). *$P < .05$ by Student *t* test. (C) Oxidative burst of WT and *Vav3*$^{-/-}$ Mϕ upon phagocytosis of apoptotic WT or *Vav3*$^{-/-}$ PMN measured at 3 hours and expressed as the increase in fluorescence intensity of oxidized carboxy H_2DCFDA. Data representative for at least 2 different experiments is given in RFU (relative fluorescence units) as scatter plot. Each symbol represents triplicate measurements, Mϕ derived from 3 different mice of each genotype (n = 3). Bars indicate medians. *$P < .05$ by Student *t* test. (D) Representative macroscopic pictures of wounds derived from WT and *Vav3*$^{-/-}$ mice at days 5 and 7 after wounding and repetitive injection with a physiologic concentration of rhTGF-β_1 (TGF-β_1^+) or of NaCl (TGF-β_1^-). (E) Statistical analysis of 16 wound areas expressed as percentage of the initial (day 0) wound size. Results presented as scatter plots. Bars indicate medians of each cohort (n = 4). *$P < .05$ by Mann-Whitney test. (F) Western blot analysis of snap-frozen wound tissue equilibrated to total actin and vimentin levels to assess expression levels of αSMA, TGFβ-RII and PECAM-1 in wound margins of different genotypes at different time points after injection of either rhTGF-β_1 (TGF-β_1+) or of NaCl (TGF-β_1-). (G) Quantification of PECAM-1$^+$ cells in 10 high power fields (HPF) of 5- and 7-day-old wounds of WT, *Vav3*$^{-/-}$ and TGF-β_1–treated *Vav3*$^{-/-}$ mice. Data are given as mean ± SD numbers of PECAM-1$^+$ cells counted per HPF. *$P < .05$ by Student *t* test. (H) Recruitment of F4/80$^+$ Mϕ assessed by FACS analysis of cells isolated by enzymatic disruption of 3- and 5-day-old wounds. Results given as scatter plots. Bars indicate the median (n = 4). *$P < .05$ by Student *t* test.

To provide evidence for a causal role of TGF-β_1 deficiency in the impaired wound closure, we injected rhTGF-β_1 (or NaCl as control) subcutaneously around the wounds as previously described.[4] Gross assessment (Figure 3D) and digital measurement (Figure 3E) of wound sizes during healing showed that local injection of rhTGF-β_1 fully rescued impaired wound healing of *Vav3*$^{-/-}$ mice. Notably, in contrast to wounds of mock-treated *Vav3*$^{-/-}$ mice with reduced αSMA, TGFβ-RII, and PECAM-1 expression, *Vav3*$^{-/-}$ wounds injected with rhTGF-β_1 showed increased myofibroblast αSMA, TGFβ-RII, and vascular PECAM-1 levels in wound lysates (Figure 3F) and increased numbers of PECAM-1$^+$ cells in wound tissue sections (Figure 3G), comparable with wounds from WT controls. Thus, in absence of Vav3, injection of rhTGF-β_1 during healing was sufficient to fully restore myofibroblast-driven wound contraction and neo-angiogenesis, unequivocally supporting a causal role for the reduced release of active TGF-β_1 in the delayed wound healing of *Vav3*$^{-/-}$ mice.

As TGF-β_1 has been reported to modulate Mϕ chemotaxis,[37] we investigated whether TGF-β_1 injection enhanced Mϕ recruitment in *Vav3*$^{-/-}$ wounds. In fact, exogenous TGF-β_1 increased the Mϕ influx only in WT, but not in *Vav3*$^{-/-}$ mice (Figure 3H), very much suggesting that TGF-β_1–induced Mϕ recruitment at wound sites distinctly depends on Vav3 and does not activate alternate emigration pathways.

Defective release of active TGF-β_1 is due to impaired adhesion with defective phagocytosis of apoptotic PMN by Mϕ in *Vav3*$^{-/-}$ mice

After cleaning the wound from invading pathogens, PMN undergo apoptosis and are removed by Mϕ by adhesion-dependent phagocytosis, which stimulates Mϕ to release large amounts of TGF-β_1.[3,4] Mϕ activation to release active TGF-β_1 (Figure S2B) preferentially depends on β_2-integrin–mediated adhesion to and phagocytosis of apoptotic PMN (Figure S2A), as also shown with β_2-integrin(CD18)$^{-/-}$ cocultures of Mϕ and PMN.[4] To analyze the adhesion-mediated phagocytosis of apoptotic PMN by Mϕ, apoptotic *Vav3*$^{-/-}$, *Vav1*$^{-/-}$/*Vav3*$^{-/-}$ and WT PMN were cocultured with *Vav3*$^{-/-}$ or WT Mϕ in all possible combinations. Mϕ-PMN conjugates were quantified using microscopy and flow cytometry after 15 minutes of coculture to assess PMN adhesion to Mϕ and after 45 minutes to assess Mϕ phagocytosing PMN. Adhesion of *Vav3*$^{-/-}$ Mϕ to apoptotic WT PMN was severely impaired, and this defect was not further reduced by coculture of *Vav3*$^{-/-}$ Mϕ with

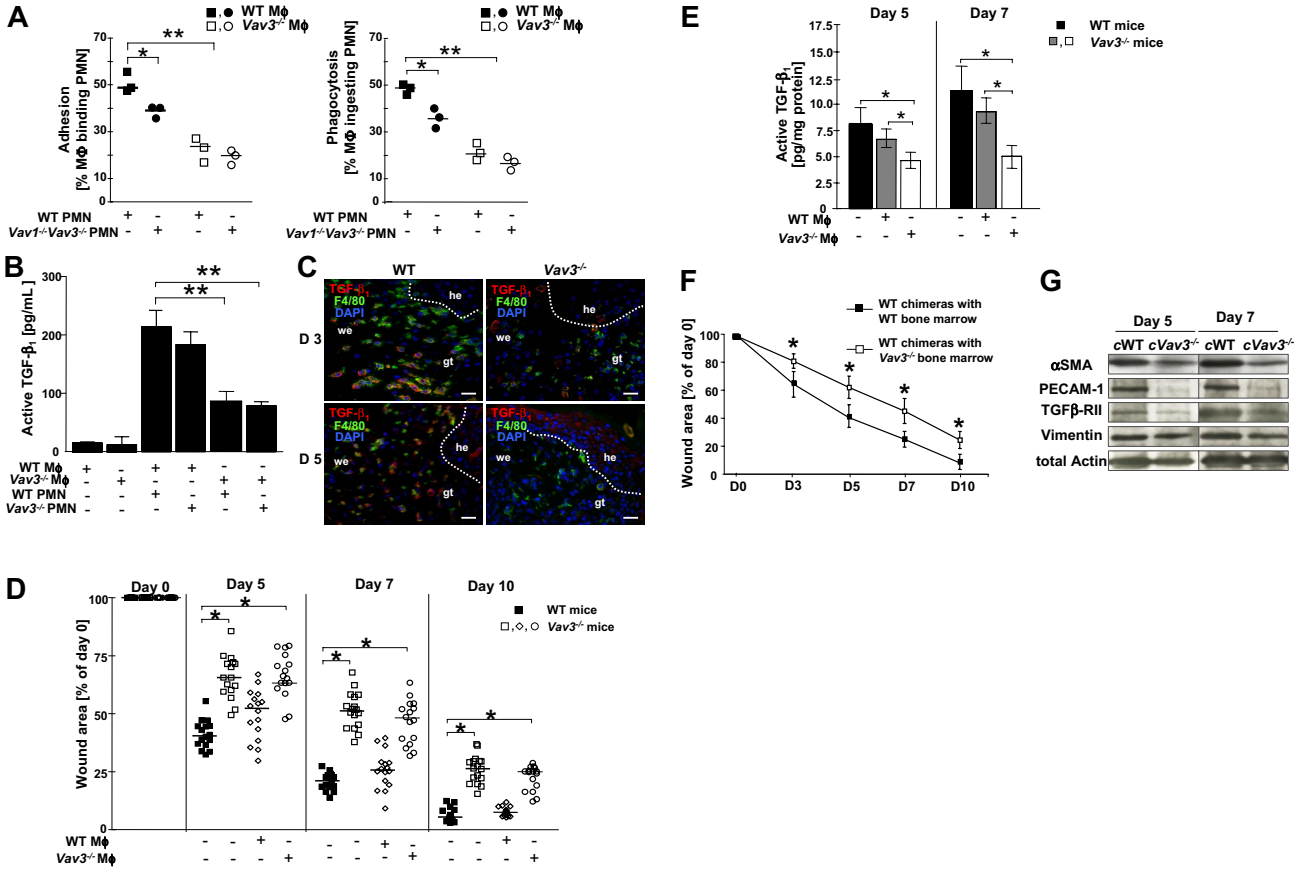

Figure 4. Defective release of active TGF-β_1 is due to impaired adhesion resulting in defective phagocytosis of apoptotic PMN by macrophages in *Vav3*$^{-/-}$ mice. (A) In vitro adhesion and phagocytosis of WT and *Vav3*$^{-/-}$ Mϕ cocultured with CMRA-labeled *Vav1*$^{-/-}$/*Vav3*$^{-/-}$ or WT apoptotic PMN for 15 minutes (adhesion; left panel) or 45 minutes (phagocytosis; right panel) assessed by flow cytometry as CMRA$^+$F4/80$^+$ conjugates. Results are expressed as percentages of PMN-binding Mϕ of the total Mϕ count (PMN-binding Mϕ × 100/total number of Mϕ). Each symbol indicates the median of a triplicate analysis. *$P < .05$; **$P < .005$. (B) Active TGF-β_1 concentrations measured by ELISA in supernatants of unstimulated WT and *Vav3*$^{-/-}$ Mϕ and in cocultures between Mϕ and PMN of the indicated genotypes. Data given as mean ± SD (n = 4). **$P < .005$. (C) Active TGF-β_1–producing Mϕ (yellow) identified by immunostaining of cryosections from 3- and 5-day-old *Vav3*$^{-/-}$ and WT wounds for TGF-β_1 (red) and F4/80 (green). Cell nuclei are counterstained with DAPI (blue; original magnification ×20, scale bar indicates 150 μm; he, hyperproliferative epidermis; we, wound edge; and gt, granulation tissue). (D) Statistical analysis of 16 wounds derived from WT mice and from *Vav3*$^{-/-}$ mice after wounding and injection of viable WT Mϕ (WT Mϕ$^+$) or of *Vav3*$^{-/-}$ Mϕ (*Vav3*$^{-/-}$ Mϕ$^+$). Wound areas are expressed as percentages of the initial (day 0) wound size. Results represented as scatter plots. Bars indicate medians of each cohort (n = 4). *$P < .05$ by Mann-Whitney test. (E) Quantitative evaluation of active TGF-β_1 measured by specific ELISA in lysates of 5- and 7-day-old wounds of WT mice and *Vav3*$^{-/-}$ mice after wounding and injection of viable WT Mϕ (WT Mϕ+) or *Vav3*$^{-/-}$ Mϕ (*Vav3*$^{-/-}$ Mϕ+) into wound margins. Results representative of 2 independent experiments are expressed as mean plus or minus SD (n = 4). *$P < .05$ by Student *t* test. (F) Lethally irradiated WT mice reconstituted with bone marrow from *Vav3*$^{-/-}$ mice reveal a significant delay in wound healing. Statistical analysis of 16 wounds per studied time point derived from lethally irradiated WT mice reconstituted with bone marrow from either WT (■) or *Vav3*$^{-/-}$ (□) mice were subjected to image analysis. Wound areas are expressed as percentages of the initial (day 0) wound size. Results given as mean ± SD (n = 4) reflect 1 of 2 independent experiments. *$P < .05$ by Mann-Whitney test. (G) Western blot analysis of expression levels of αSMA, TGFβ-RII and PECAM-1 equilibrated to total actin and vimentin levels in wound margins of WT and *Vav3*$^{-/-}$ bone marrow chimeric mice at days 5 and 7 after wounding (cWT, WT chimera with WT bone marrow; *cVav3*$^{-/-}$, WT chimera with *Vav3*$^{-/-}$ bone marrow).

Vav3$^{-/-}$ PMN (Figure 4A and data not shown). Instead, when coculturing WT Mϕ with *Vav1*$^{-/-}$/*Vav3*$^{-/-}$ PMN, a minor, though significant, decrease in adhesion was observed. These data suggest that Vav3 deficiency in Mϕ is predominantly responsible for the observed adhesion defect, whereas in PMN a double Vav1/Vav3 deficiency is required to affect adhesion to some extent. In fact, previous reports confirm that Vav1 and Vav3 play redundant roles in PMN adhesion and spreading, functions that are only impaired by double deficiency.[28]

Firm adhesion of target cells to phagocytes markedly contributes to phagocytic efficacy.[4,14,38] Indeed, we observed a defective phagocytosis of apoptotic WT or *Vav3*$^{-/-}$ PMN by *Vav3*$^{-/-}$ Mϕ, at least partly caused by the impaired physical attachment of apoptotic PMN to Mϕ (Figure 4A). Similar to the defective adhesion, coculture of *Vav1*$^{-/-}$/*Vav3*$^{-/-}$ PMN with WT Mϕ moderately reduced PMN engulfment. *Vav3*$^{-/-}$ and WT Mϕ engulfed identical amounts of latex beads (data not shown), suggesting that the phagocytic machinery itself is functional, and that Vav3 deficiency specifically affected phagocytosis of apoptotic PMN by *Vav3*$^{-/-}$ Mϕ.

Next, we cocultured Mϕ with apoptotic PMN for 24 hours to assess the supernatants for concentrations of active TGF-β_1 by ELISA (Figure 4B). WT or *Vav3*$^{-/-}$ Mϕ cultivated in the absence of PMN, as well as cultures of viable PMN with either genotype of Mϕ rendered negligible amounts of TGF-β_1, whereas high concentrations of active TGF-β_1 of approximately 215 pg/mL were found in supernatants of WT Mϕ/PMN cocultures. Active TGF-β_1 decreased significantly to below 100 pg/mL after coculture of *Vav3*$^{-/-}$ Mϕ with either WT or *Vav3*$^{-/-}$ PMN, very much suggesting that Vav3 deficiency in Mϕ predominantly contributes to defective adhesion-dependent phagocytosis of apoptotic PMN by Mϕ, with significantly decreased active TGF-β_1.

The finding that TGF-β_1 concentrations particularly depend on Vav3 expression in Mϕ was confirmed by immunostaining in vivo, with lower numbers of F4/80$^+$ TGF-β_1-producing Mϕ present at

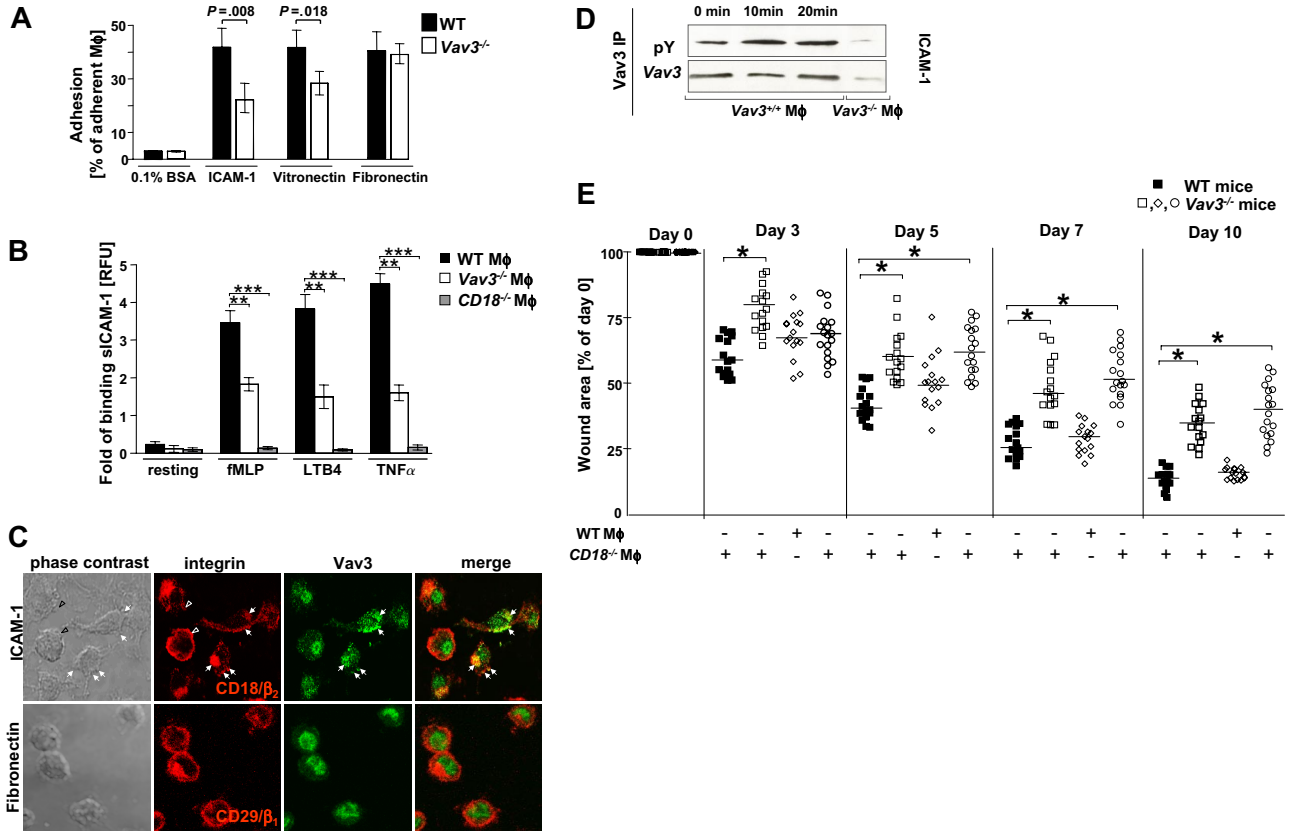

Figure 5. Vav3 is a downstream target of β_2-integrin–dependent macrophage adhesion. (A) Adherence of TNFα-stimulated, CMFDA-loaded WT and *Vav3*$^{-/-}$ Mϕ plated onto β_1-integrin (fibronectin)–, β_2-integrin (ICAM-1)–, or β_3-integrin (vitronectin)–specific ligands or on 0.1% BSA as control is expressed as percentage of adherent Mϕ related to input cells measured after 15 minutes of incubation. Representative results for 3 independent experiments are shown as mean ± SD (n = 3). *P* assessed by Student *t* test. (B) Binding of soluble ICAM-1/Fc-FITC by unstimulated (resting) or fMLP-, LTB4- and TNFα-stimulated WT, *Vav3*$^{-/-}$ and *CD18*$^{-/-}$ Mϕ. Results are given in RFU, representing the ratio between the mean green fluorescence intensities of Mϕ incubated with ICAM-1/Fc and Mϕ incubated with human IgG for each stimulation. Bars indicate means ± SD of triplicate measurements and are representative for 3 different experiments. $^{**}P < .005$; $^{***}P < .001$ by Student *t* test. (C) Confocal microscopy of WT Mϕ plated for 15 minutes on ICAM-1 (top panel) revealed β_2 integrins (CD18) (red) clustering at focal adhesion sites (open and filled arrows). Vav3 (green) colocalized with CD18 in more than 60% of the plated Mϕ within the focal adhesion contacts (filled arrows). Colocalization is indicated by the yellow staining. No colocalization occurred between Vav3 and CD29 upon plating Mϕ onto fibronectin (bottom panel). (D) Vav3 phosphorylation detected by Vav3 immunoprecipitation and subsequent blotting against anti-phosphotyrosine antibody (pY) induced 10 minutes or 20 minutes after plating Mϕ on ICAM-1–coated plates. Total Vav3 levels served as loading controls, *Vav3*$^{-/-}$ Mϕ served as technical controls. Data are representative of at least 3 independent experiments. (E) Injection of *β2-integrin* (*CD18*)$^{-/-}$ Vav3 competent Mϕ into wound margins of *Vav3*$^{-/-}$ mice does not rescue the wound healing defect. WT or *CD18*$^{-/-}$ bone marrow–derived Mϕ were injected at 4 sites into wound margins of *Vav3*$^{-/-}$ mice. Statistical analysis of 16 wounds of each studied time point derived from WT mice or from *Vav3*$^{-/-}$ mice after wounding and injection of viable WT Mϕ (WT Mϕ) or *CD18*$^{-/-}$ Mϕ (*CD18*$^{-/-}$ Mϕ^{+}). Wound areas are expressed as percentages of the initial (day 0) wound size. Results represented as scatter plots. Bars indicate medians of each cohort (n = 4). $^{*}P < .05$ by Mann-Whitney test.

Vav3$^{-/-}$ wound edges at days 3 and 5 after wounding, by contrast with high numbers of F4/80^{+} TGF-β_1–producing Mϕ at WT wound sites (Figure 4C).

To differentiate whether reduced Mϕ recruitment, or rather their impaired phagocytic function with reduced release of active TGF-β_1 were causal for the impaired wound healing in Vav3 deficiency, we next injected WT or *Vav3*$^{-/-}$ Mϕ subcutaneously directly in the wound margins of *Vav3*$^{-/-}$ and WT mice at day 2 after wounding, thus circumventing the *Vav3*$^{-/-}$ Mϕ transmigration defect. Before injection, viability and proper functions of Mϕ were confirmed by Trypan blue exclusion, appropriate phagocytosis of apoptotic PMN and robust interleukin-12 (IL-12) release upon maximal stimulation (data not shown). Notably, injection of WT Vav3-competent Mϕ in wound margins of *Vav3*$^{-/-}$ mice significantly increased the level of active TGF-β_1 at days 5 and 7 after wounding (Figure 4E), accelerated wound closure at day 5 and fully rescued the wound healing of *Vav3*$^{-/-}$ mice by day 10. By contrast, injection of *Vav3*$^{-/-}$ Mϕ in *Vav3*$^{-/-}$ wound margins failed to increase active TGF-β_1 levels and to rescue impaired wound healing (Figure 4D,E), clearly indicating the requirement for Vav3 in Mϕ for phagocytic uptake of PMN and subsequent release of active TGF-β_1, eventually promoting proper wound healing.

To further confirm the exclusive requirement for Vav3 in leukocytes, but not in other cells for tissue repair, we next studied wound healing of lethally irradiated WT mice reconstituted with WT or *Vav3*$^{-/-}$ bone marrow. Notably, Vav3-competent mice reconstituted with *Vav3*$^{-/-}$ bone marrow displayed a delay in wound healing similar to that observed for *Vav3*$^{-/-}$ mice (Figure 4F). Moreover, compared with WT control chimeras, wounds from *Vav3*$^{-/-}$ chimeras showed reduced myofibroblast differentiation and impaired angiogenesis as assessed by αSMA, TGFβ-RII, and PECAM-1 expression in tissue lysates (Figure 4G), confirming that Vav3 deficiency exclusively in leukocytes is causal for the impaired wound healing.

Collectively, wild-type levels of Vav3 in Mϕ are essential for proper wound healing and, if absent, result in defective phagocytosis of apoptotic PMN by Mϕ with reduced oxidative burst and reduced release of active TGF-β_1, impaired myofibroblasts-driven wound closure, and neo-angiogenesis. The delayed wound healing phenotype of *Vav3*$^{-/-}$ mice closely resembles that observed in

LAD1 patients and *CD18*$^{-/-}$ mice,[4] and neither *Vav3*$^{-/-}$ nor *CD18*$^{-/-}$ Mϕ injected into wound margins of *Vav3*$^{-/-}$ mice could rescue the wound healing defect (Figures 4D, 5E). This may indicate that CD18 deficiency and Vav3 deficiency result in identical defects in Mϕ and, thus, suggest that CD18 and Vav3 are within the same signaling pathway controlling engulfment of PMN by Mϕ and active TGF-β_1 release. Therefore, we set out to further investigate whether Vav3 may qualify as a downstream target in the β_2-integrin (CD18)–dependent signaling in Mϕ.

Vav3 is a downstream target of β_2-integrin–dependent Mϕ adhesion

As the physical attachment of Mϕ to apoptotic PMN depends on β_2-integrins, we studied the adhesive property of WT and *Vav3*$^{-/-}$ Mϕ onto the β_2-integrin ligand intercellular adhesion molecule 1 (ICAM-1), which mediates β_2-integrin–dependent formation of the phagocytic synapse[4] (Figure S2A). Integrin-mediated Mϕ activation was achieved by TNFα stimulation before plating on defined ligands. Comparable CD18 expression levels were confirmed for WT and *Vav3*$^{-/-}$ Mϕ and PMN before and after TNFα stimulation as assessed by flow cytometry (Figure S2D and data not shown). Notably, *Vav3*$^{-/-}$ Mϕ revealed a significantly reduced adhesion to ICAM-1 compared with WT Mϕ. This Vav3-dependent β_2-integrin–mediated adhesion to ICAM-1 was specific, as adhesion of both WT and *Vav3*$^{-/-}$ Mϕ to BSA was insignificant. Compared with the β_2-integrin–dependent reduced adhesion to ICAM-1, a minor, but significant decrease in adhesion was detected when *Vav3*$^{-/-}$ Mϕ were plated onto the β_3-integrin ligand vitronectin, indicating that Vav3, at least in part, controls β_3-integrin–dependent Mϕ adhesion. This finding is in line with previous reports indicating Vav3 to control $\alpha_v\beta_3$–dependent polarization and spreading of osteoclasts.[32] By contrast, Vav3 deficiency did not affect β_1-integrin–mediated binding to fibronectin, suggesting that Vav3 is preferentially responsible for β_2-integrin–mediated Mϕ adhesion and, to a lesser extent, contributes to β_3-integrin–mediated Mϕ adhesion (Figure 5A).

Moreover, these findings suggested a role for Vav3 in β_2-integrin–dependent strengthening of the synapse between Mϕ and PMN, which depends on ICAM-1 binding. To investigate the contribution of Vav3 to β_2-integrin activation in more detail, we assessed β_2-integrin affinity of WT, *Vav3*$^{-/-}$ and *CD18*$^{-/-}$ Mϕ by their capacity to bind soluble ICAM-1 (sICAM-1). Activated WT Mϕ bound sICAM-1 up to 4 times more efficiently compared with unstimulated or to *CD18*$^{-/-}$ Mϕ. Remarkably, in the absence of Vav3 the capacity of Mϕ to bind sICAM-1 was diminished to 50% when stimulated with fMLP and to 30% when activated by TNFα (Figure 5B). These results strongly suggest that Vav3 controls integrin affinity upon activation and thus regulates the extent of outside-in signaling required for firm adhesion, phagocytosis and oxidative burst.

To further characterize the role of Vav3 as a downstream target of β_2-integrin–dependent signaling in Mϕ, we analyzed the cellular localization of Vav3 and CD18 during Mϕ adhesion on ICAM-1 using confocal microscopy. CD18 (Figure 5C second top panel, red) redistributed and clustered within focal adhesion contacts (Figure 5C second top panel, open arrows) at the cell membrane when Mϕ were plated onto the β_2-integrin specific ligand ICAM-1, which is also present in the phagocytic synapse (Figure 5C). In more than 60% of the Mϕ, Vav3 (Figure 5C third top panel, green) colocalized with CD18 at focal adhesion sites as revealed by the yellow staining indicated with filled arrows (Figure 5C fourth top panel). In contrast, no stringent colocalization of CD29 (β_1-integrins) with Vav3 was observed when Mϕ were plated onto fibronectin (Figure 5C bottom panels), suggesting that Vav3 is not involved in the β_1-integrin–dependent adhesion, but in the β_2-integrin–dependent adhesion to ICAM-1 and, thus, in the phagocytic cup formation.

Activation of Vav proteins requires phosphorylation of specific tyrosine residues as a prerequisite to activate downstream targets. So far, integrin signaling via Vav3 has rarely been addressed in Mϕ.[31,32] To study whether Vav3 is activated in response to β_2-integrin engagement, the phosphorylation status of Vav3 after Mϕ binding to ICAM-1 was assessed. Before adhesion, Mϕ were treated with TNFα to enhance integrin adhesive activity. No phosphorylation occurred upon TNFα treatment when Mϕ were plated on BSA-coated dishes, excluding any direct effect of TNFα on the phosphorylation status of Vav3 (data not shown). Induction of Vav3 phosphorylation was observed at 10 minutes after plating Mϕ onto ICAM-1, whereas the level of total Vav3 remained unchanged (Figure 5D).

Additional evidence for the β_2-integrin–dependent Vav3 activation was provided by the observation that *CD18*hypomorphic Mϕ (with only 15% of CD18 WT expression levels[39]) revealed significantly reduced Vav3 phosphorylation upon adherence on ICAM-1, whereas *CD18*$^{-/-}$ Mϕ attached poorly and could not be harvested in sufficient quantities (unpublished data).

These data, together with the finding that, similar to injection of *Vav3*$^{-/-}$ Mϕ, injection of *CD18*$^{-/-}$ Mϕ in wound margins does not restore the impaired wound healing of *Vav3*$^{-/-}$ mice (Figure 5E), suggest that Vav3 in Mϕ constitutes a key molecule in the β_2-integrin–dependent formation of a functional phagocytic synapse essentially required for proper wound healing.

Discussion

We here found Vav3 proteins to be specifically required for proper healing of cutaneous full-thickness wounds, whereas their absence results in delayed angiogenesis and impaired wound closure. This phenotype closely resembles nonhealing wounds in LAD1 patients with functional mutations in the *CD18* gene[16,40] and *CD18*$^{-/-}$ mice.[4] The impaired wound closure in *Vav3*$^{-/-}$ mice is essentially due to a β_2-integrin–dependent deficient formation of the phagocytic synapse between *Vav3*$^{-/-}$ Mϕ and apoptotic PMN. The defective engulfment of PMN leads to reduced release of active TGF-β_1 from Mϕ, which in turn is responsible for defective myofibroblast-driven wound contraction and reduced angiogenesis. Injection of either recombinant TGF-β_1 or Vav3 competent Mϕ into wound margins of *Vav3*$^{-/-}$ mice fully rescued the defective wound healing.

We here identified a previously unrecognized role for Vav3 in Mϕ, linking to a central role for Vav3 in β_2-integrin downstream signaling in Mϕ, which, if defective, may contribute to disturbances in tissue repair and host defense in general. In particular, between days 5 and 7 after wounding, the phase of granulation tissue contraction and neo-angiogenesis, *Vav3*$^{-/-}$ wounds were significantly larger compared with WT wounds. Reduced αSMA and TGFβ-RII expression in *Vav3*$^{-/-}$ granulation tissue suggest that, similar to CD18 deficiency,[4] impaired wound closure in *Vav3*$^{-/-}$ mice results from reduced myofibroblasts differentiation. Myofibroblasts differentiation is characterized by the de novo expression of αSMA, conferring wound contraction in vivo[41] and in vitro.[42,43] TGF-β_1 is the major growth factor inducing αSMA$^+$myofibroblast differentiation[44] through specific binding to TGFβ-RII.[45] TGF-β_1 amplifies its response via an autocrine

mechanism with up-regulation of TGFβ-RII and enhanced release of active TGF-β_1 from myofibroblasts and inflammatory cells. Therefore, decreased TGF-β_1 release from Mϕ in the initial phases of wound healing will result in substantially amplified effects on myofibroblasts differentiation and angiogenesis[5,44] driving tissue repair. We here demonstrate that reduced active TGF-β_1 in granulation tissue of *Vav3*$^{-/-}$ mice is the major pathogenic event in impaired wound healing, since wound contraction is fully rescued after subcutaneous injection of rhTGF-β_1. TGF-β_1 release from Mϕ is essentially induced upon phagocytosis of apoptotic PMN at wound sites.[3,4] As both PMN and Mϕ are mandatory for the formation of the phagocytic synapse with sufficient TGF-β_1 release, we studied their emigration patterns.

Mϕ recruitment at wound sites was reduced in Vav3 deficiency; however, the recruitment defect was similar in *Vav3*$^{-/-}$ and *Vav1*$^{-/-}$; *Vav3*$^{-/-}$ mice, suggesting that Vav3 alone is critical for the Mϕ extravasation to wound sites. This is in line with previous data reporting Vav3 to control cytoskeleton organization, polarization and spreading of Mϕ[32] or MCS-F-induced Mϕ chemotaxis,[46] all critical functions for Mϕ emigration. Irrespective of the underlying mechanism, defective Mϕ recruitment was not causal for the impaired wound healing in *Vav3*$^{-/-}$ mice, as circumventing this defect by injection of *Vav3*$^{-/-}$ Mϕ directly into the wound margin failed to rescue the healing disturbance. However, differences in the recruitment of Mϕ and PMN between *Vav3*$^{-/-}$ and the β_2-integrin(*CD18*)$^{-/-}$ mice may explain the earlier onset of the wound healing delay in *Vav3*$^{-/-}$ mice compared with *CD18*$^{-/-}$ mice (see also "Discussion" section of online data supplement).

In this report, we define the defective formation of the phagocytic synapse between *Vav3*$^{-/-}$ Mϕ and apoptotic PMN as the major cause for the reduced release of active TGF-β_1 and the resulting wound healing deficiency. In fact, injection of *Vav3*$^{-/-}$ Mϕ directly into *Vav3*$^{-/-}$ wound margins failed to restore the impaired wound closure. In contrast, injection of WT Mϕ fully restored the wound defect and the diminished TGF-β_1 in *Vav3*$^{-/-}$ mice at levels comparable with WT mice, clearly demonstrating that Vav3 deficiency in Mϕ with impaired adhesion-dependent phagocytosis of apoptotic PMN is causal for the wound healing defect in *Vav3*$^{-/-}$ mice.

Phagocytosis of apoptotic PMN by Mϕ and the concomitant release of active TGF-β_1 were significantly reduced in absence of Vav3 in Mϕ, but not in PMN. Even Vav1/Vav3 double deficiency in PMN cocultured with WT Mϕ reduced the phagocytic cup formation only moderately, but to much lower extent compared with *Vav3*$^{-/-}$ Mϕ cocultured with WT PMN. Because adhesion of target cells to phagocytes before engulfment contributes to the efficacy of cell uptake,[4,14,38] the impaired attachment between PMN and *Vav3*$^{-/-}$ Mϕ may account for the disturbed phagocytosis. Thus, Vav3 is essentially required in Mϕ for efficient cell-cell contacts and thus promotes engulfment of apoptotic PMN by Mϕ. Vav3 deficiency leads to the inefficient Mϕ-PMN attachment and impaired PMN uptake, resulting in reduced release of active TGF-β_1 from Mϕ. Possibly, the diminished oxidative burst in *Vav3*$^{-/-}$ Mϕ upon phagocytosis of apoptotic PMN contributes to the reduced TGF-β_1 activation and consequences thereof. In fact, activation of TGF-β_1 has been reported to be mediated by ROS,[36] and VaV guanin nucleotide exchange factors link integrin-mediated signaling with the assembly of the nicotinamid-adenin dinucleotide phosphate oxidase complex responsible for the production of ROS in Mϕ.[47]

The almost identical phenotypes with delayed wound closure, defective phagocytic synapse formation and reduced release of active TGF-β_1 in *CD18*$^{-/-}$ and *Vav3*$^{-/-}$ mice very much suggest that β_2-integrins may preferentially control these key steps via the guanine exchange factor Vav3 in Mϕ. Several lines of evidence support this view.

First, β_2-integrins are mandatory for the attachment-mediated phagocytosis of PMN by Mϕ and for the phagocytic synapse formation. For this, binding of Mac-1 (CD11b/CD18) on Mϕ to its counterreceptor ICAM-1 on PMN and vice versa are essential.[4] In case Vav3 constituted a downstream target of CD18, we predicted that *Vav3*$^{-/-}$ Mϕ would display reduced adhesion to ICAM-1. And exactly that is what we found. By contrast, *Vav3*$^{-/-}$ Mϕ adhesion onto fibronectin, a β_1-integrin–dependent ligand, was not altered, strongly suggesting a critical role for Vav3 in β_2-integrin–dependent Mϕ adhesion. Even though we found a decrease in adhesion of *Vav3*$^{-/-}$ Mϕ to the β_3-integrin ligand vitronectin, suggesting that Vav3 plays a role in β_3-integrin signaling. Vitronectin is an extracellular matrix protein that does not occur at the synapse between Mϕ and apoptotic PMN, and thus may not be relevant in the phagocytic cup formation studied here. In fact, β_3-integrins/CD36 complexes interact with unknown moieties on PMN via a thrombospondin bridge.[48]

In support of Vav3 preferentially relaying β_2-integrin–mediated signals, Vav3 distinctly controlled the Mϕ capacity to bind β_2-integrin–specific ligands upon activation, as *Vav3*$^{-/-}$ Mϕ presented a severely reduced capacity to bind sICAM-1 compared with WT Mϕ. In contrast to this finding, a previous report on phagocytosis of complement-opsonized red blood cells by *Vav3*$^{-/-}$ and *Vav1*$^{-/-}$*Vav3*$^{-/-}$ Mϕ indicated that Vav3 alone has no effect on β_2-integrin–mediated phagocytosis and that even the Vav1/Vav3 double deficiency does not impair β_2-integrin–mediated adhesion to Mϕ.[31] However, this study investigated rapid phagocytosis of C3-biopsonized particles by Mϕ previously stimulated with PMA, which is known to directly activate the protein kinase C required for complement-mediated phagocytosis.[49] This may have completely compensated for the absence of upstream Vav proteins during adhesion and may have partially compensated for the lack of Vav3 during β_2-integrin–dependent phagocytosis. We here studied binding of sICAM-1 to Mϕ stimulated with fMLP, LTB4, or TNFα, which initiate a high-affinity ICAM-1–binding state for β_2-integrins.[50] Our experimental approach using a physiologic ligand (ICAM-1) and macrophage stimuli occurring in a variety of inflammatory conditions closely reflects the adhesion-dependent phagocytosis of apoptotic PMN during wound healing, and these conditions may additionally require Vav3 signaling.

Second, binding of WT Mϕ to ICAM-1, the major ligand for Mac-1 in the phagocytic synapse resulted in the phosphorylation of Vav3, essentially required for Vav3 exchange activity and activation of Rho-GTPases. Vav3 phosphorylation in response to macrophage adhesion to ICAM-1 was reduced in macrophages with reduced CD18 expression, further strengthening the role of Vav3 as a potential downstream target of β_2-integrin–dependent signaling.

Third, colocalization of CD18 and Vav3 specifically occurred in Mϕ upon adhesion to ICAM-1 but not to fibronectin.

Fourth, apart from the almost exact recapitulation of the wound healing phenotype of *CD18*$^{-/-}$ mice with deficient phagocytic cup formation, reduced release of active TGF-β_1 and impaired myofibroblast-driven wound contraction, *Vav3*$^{-/-}$ mice exhibit spontaneous ulcerations, as earlier reported for *CD18*$^{-/-}$ mice.[10]

Finally and most importantly, injection of either *Vav3*$^{-/-}$ or *CD18*$^{-/-}$ Mϕ into wound margins failed to rescue the wound healing defect of *Vav3*$^{-/-}$ mice. These data unequivocally support a critical role for Vav3 as a downstream target in β_2-integrin–dependent signaling. However, the β_2-integrins–Vav3 axis may not

exclusively mediate phagocytic synapse formation, engulfment of apoptotic PMN, and release of active TGF-β_1 from Mϕ, but other receptors may play a role.[51] At least, inhibition of β_3-integrins resulted in a significant, though—compared with blocking the CD18 or ICAM-1 function—markedly lesser decrease in adhesion-dependent phagocytosis of apoptotic PMN and a milder impairment of active TGF-β_1 release by Mϕ in vitro. These data suggest β_2-integrins to preferentially, but not exclusively control these processes. Even though β_3-integrins most likely contribute to the phagocytosis of apoptotic PMN and Mϕ in vitro, their in vivo role is unclear. In contrast to a severe wound healing defect in β_2-integrin(*CD18*)$^{-/-}$ mice and LAD1 patients[15] due to a decrease in active TGF-β_1,[4] *β_3-integrin*$^{-/-}$ mice were reported to present accelerated wound healing and enhanced TGF-β_1 release and signaling.[52]

Our data show that Vav3 cell-specifically relays β_2-integrin signaling, thus fine-tuning distinct cellular functions. Although Vav3 is not required for β_2-integrin–dependent PMN functions, it is distinctly required for Mϕ recruitment and their capacity to build the phagocytic synapse efficiently. There has been a recent focus on targeting signaling molecules as an approach to modulate and rebalance inflammation in vivo.[53] Targeting Vav3 in Mϕ by agonists or antagonists may specifically modulate Mϕ recruitment and phagocytosis of apoptotic PMN with subsequent modulation of TGF-β_1 release, while preserving PMN recruitment, a strategy that would minimize overall immune suppression. Alternatively, as enhanced TGF-β_1 release from activated Mϕ is pathogenic in a variety of fibrotic conditions[54] including hypertrophic scar and keloid formation, targeting of Vav3 may be particularly beneficial for these difficult-to-treat conditions.

Acknowledgments

We thank Heidi Hainzl, Henriette Peter, and Carmen Hauser for excellent technical assistance.

K.S.-K., A.S., K.L.R., A.G., C.S., and K.D.F. are supported by Deutsche Forschungsgemeinschaft (DFG) grants SFB497-C7 (K.S.-K., A.S.), KFO142 (K.S.-K.), SFB497-C11 (K.L.R., A.G.), DFG SU195/3-1 (C.S.), and SFB497-C6 (K.D.F.).

Authorship

Contribution: A.S. and T.P. designed and performed research, analyzed data, and wrote the manuscript; J.S., T.O., H.W., F.M., M.W., C.S., and B.W. designed research and analyzed data; A.G., K.L.R., X.R.B., and K.D.F. provided research tools, designed research and analyzed data; and K.S.-K. designed research and analyzed data, and wrote the manuscript.

Conflict-of-interest disclosure: The authors declare no competing financial interests.

Correspondence: Karin Scharffetter-Kochanek, MD, Department of Dermatology and Allergic Diseases, University of Ulm, Maienweg 12, 89081 Ulm, Germany; e-mail: karin.scharffetter-kochanek@uniklinik-ulm.de.

References

1. Martin P. Wound healing—aiming for perfect skin regeneration [review]. Science. 1997;276:75-81.
2. Singer AJ, Clark RA. Cutaneous wound healing. N Engl J Med. 1999;341:738-746.
3. Fadok VA, Bratton DL, Konowal A, Freed PW, Westcott JY, Henson PM. Macrophages that have ingested apoptotic cells in vitro inhibit proinflammatory cytokine production through autocrine/paracrine mechanisms involving TGF-beta, PGE2, and PAF. J Clin Invest. 1998;101:890-898.
4. Peters T, Sindrilaru A, Hinz B, et al. Wound-healing defect of CD18(−/−) mice due to a decrease in TGF-beta1 and myofibroblast differentiation. Embo J. 2005;24:3400-3410.
5. Roberts AB, Sporn MB, Assoian RK, et al. Transforming growth factor type beta: rapid induction of fibrosis and angiogenesis in vivo and stimulation of collagen formation in vitro. Proc Natl Acad Sci U S A. 1986;83:4167-4171.
6. Springer TA, Anderson DC. Leukocyte complement receptors and adhesion proteins in the inflammatory response: insights from an experiment of nature. Biochem Soc Symp. 1986;51:47-57.
7. Arnaout MA. Structure and function of the leukocyte adhesion molecules CD11/CD18. Blood. 1990;75:1037-1050.
8. Chiriac MT, Roesler J, Sindrilaru A, Scharffetter-Kochanek K, Zillikens D, Sitaru C. NADPH oxidase is required for neutrophil-dependent autoantibody-induced tissue damage. J Pathol. 2007;212:56-65.
9. Mizgerd JP, Kubo H, Kutkoski GJ, et al. Neutrophil emigration in the skin, lungs, and peritoneum: different requirements for CD11/CD18 revealed by CD18-deficient mice. J Exp Med. 1997;186:1357-1364.
10. Scharffetter-Kochanek K, Lu H, Norman K, et al. Spontaneous skin ulceration and defective T cell function in CD18 null mice. J Exp Med. 1998;188:119-131.
11. Sindrilaru A, Seeliger S, Ehrchen JM, et al. Site of blood vessel damage and relevance of CD18 in a murine model of immune complex-mediated vasculitis. J Invest Dermatol. 2007;127:447-454.
12. Liu Z, Zhao M, Li N, Diaz LA, Mayadas TN. Differential roles for beta2 integrins in experimental autoimmune bullous pemphigoid. Blood. 2006;107:1063-1069.
13. Auffray C, Fogg D, Garfa M, et al. Monitoring of blood vessels and tissues by a population of monocytes with patrolling behavior. Science. 2007;317:666-670.
14. Mevorach D, Mascarenhas JO, Gershov D, Elkon KB. Complement-dependent clearance of apoptotic cells by human macrophages. J Exp Med. 1998;188:2313-2320.
15. Bunting M, Harris ES, McIntyre TM, Prescott SM, Zimmerman GA. Leukocyte adhesion deficiency syndromes: adhesion and tethering defects involving beta 2 integrins and selectin ligands. Curr Opin Hematol. 2002;9:30-35.
16. Bowen TJ, Ochs HD, Altman LC, et al. Severe recurrent bacterial infections associated with defective adherence and chemotaxis in two patients with neutrophils deficient in a cell-associated glycoprotein. J Pediatr. 1982;101:932-940.
17. Mocsai A, Abram CL, Jakus Z, Hu Y, Lanier LL, Lowell CA. Integrin signaling in neutrophils and macrophages uses adaptors containing immunoreceptor tyrosine-based activation motifs. Nat Immunol. 2006;7:1326-1333.
18. Schymeinsky J, Mocsai A, Walzog B. Neutrophil activation via beta2 integrins (CD11/CD18): molecular mechanisms and clinical implications. Thromb Haemost. 2007;98:262-273.
19. Bustelo XR. Regulatory and signaling properties of the Vav family. Mol Cell Biol. 2000;20:1461-1477.
20. Turner M, Billadeau DD. VAV proteins as signal integrators for multi-subunit immune-recognition receptors. Nat Rev Immunol. 2002;2:476-486.
21. Fischer KD, Tedford K, Penninger JM. Vav links antigen-receptor signaling to the actin cytoskeleton. Semin Immunol. 1998;10:317-327.
22. Holsinger LJ, Graef IA, Swat W, et al. Defects in actin-cap formation in Vav-deficient mice implicate an actin requirement for lymphocyte signal transduction. Curr Biol. 1998;8:563-572.
23. Doody GM, Bell SE, Vigorito E, et al. Signal transduction through Vav-2 participates in humoral immune responses and B cell maturation. Nat Immunol. 2001;2:542-547.
24. Tedford K, Nitschke L, Girkontaite I, et al. Compensation between Vav-1 and Vav-2 in B cell development and antigen receptor signaling. Nat Immunol. 2001;2:548-555.
25. Fujikawa K, Miletic AV, Alt FW, et al. Vav1/2/3-null mice define an essential role for Vav family proteins in lymphocyte development and activation but a differential requirement in MAPK signaling in T and B cells. J Exp Med. 2003;198:1595-1608.
26. Yron I, Deckert M, Reff ME, Munshi A, Schwartz MA, Altman A. Integrin-dependent tyrosine phosphorylation and growth regulation by Vav. Cell Adhes Commun. 1999;7:1-11.
27. Cichowski K, Brugge JS, Brass LF. Thrombin receptor activation and integrin engagement stimulate tyrosine phosphorylation of the proto-oncogene product, p95vav, in platelets. J Biol Chem. 1996;271:7544-7550.
28. Gakidis MA, Cullere X, Olson T, et al. Vav GEFs are required for beta2 integrin-dependent functions of neutrophils. J Cell Biol. 2004;166:273-282.
29. Utomo A, Cullere X, Glogauer M, Swat W, Mayadas TN. Vav proteins in neutrophils are required for FcgammaR-mediated signaling to Rac GTPases and nicotinamide adenine dinucleotide phosphate oxidase component p40(phox). J Immunol. 2006;177:6388-6397.

30. Utomo A, Hirahashi J, Mekala D, et al. Requirement for Vav proteins in post-recruitment neutrophil cytotoxicity in IgG but not Ccmplement C3-dependent injury. J Immunol. 2008;180:6279-6287.
31. Hall AB, Gakidis MA, Glogauer M, et al. Requirements for Vav guanine nucleotide exchange factors and Rho GTPases in FcgammaR- and complement-mediated phagocytosis. Immunity. 2006;24:305-316.
32. Faccio R, Teitelbaum SL, Fujikawa K, et al. Vav3 regulates osteoclast function and bone mass. Nat Med. 2005;11:284-290.
33. Sauzeau V, Sevilla MA, Rivas-Elena JV, et al. Vav3 proto-oncogene deficiency leads to sympathetic hyperactivity and cardiovascular dysfunction. Nat Med. 2006;12:841-845.
34. Gabbiani G, Hirschel BJ, Ryan GB, Statkov PR, Majno G. Granulation tissue as a contractile organ. A study of structure and function. J Exp Med. 1972;135:719-734.
35. Tomasek JJ, Gabbiani G, Hinz B, Chaponnier C, Brown RA. Myofibroblasts and mechano-regulation of connective tissue remodelling. Nat Rev Mol Cell Biol. 2002;3:349-363.
36. Barcellos-Hoff MH, Dix TA. Redox-mediated activation of latent transforming growth factor-beta 1. Mol Endocrinol. 1996;10:1077-1083.
37. Wahl SM, Hunt DA, Wakefield LM, et al. Transforming growth factor type beta induces monocyte chemotaxis and growth factor production. Proc Natl Acad Sci U S A. 1987;84:5788-5792.
38. Fallman M, Andersson R, Andersson T. Signaling properties of CR3 (CD11b/CD18) and CR1 (CD35) in relation to phagocytosis of complement-opsonized particles. J Immunol. 1993;151:330-338.
39. Wilson RW, Ballantyne CM, Smith CW, et al. Gene targeting yields a CD18-mutant mouse for study of inflammation. J Immunol. 1993;151:1571-1578.
40. Anderson DC, Smith CW. Leukocyte Adhesion Deficiencies. New York, NY: McGraw-Hill; 2001.
41. Serini G, Gabbiani G. Mechanisms of myofibroblast activity and phenotypic modulation. Exp Cell Res. 1999;250:273-283.
42. Arora PD, McCulloch CA. Dependence of collagen remodelling on alpha-smooth muscle actin expression by fibroblasts. J Cell Physiol. 1994;159:161-175.
43. Hinz B, Celetta G, Tomasek JJ, Gabbiani G, Chaponnier C. Alpha-smooth muscle actin expression upregulates fibroblast contractile activity. Mol Biol Cell. 2001;12:2730-2741.
44. Desmouliere A, Geinoz A, Gabbiani F, Gabbiani G. Transforming growth factor-beta 1 induces alpha-smooth muscle actin expression in granulation tissue myofibroblasts and in quiescent and growing cultured fibroblasts. J Cell Biol. 1993;122:103-111.
45. Cowin AJ, Holmes TM, Brosnan P, Ferguson MW. Expression of TGF-beta and its receptors in murine fetal and adult dermal wounds. Eur J Dermatol. 2001;11:424-431.
46. Vedham V, Phee H, Coggeshall KM. Vav activation and function as a rac guanine nucleotide exchange factor in macrophage colony-stimulating factor-induced macrophage chemotaxis. Mol Cell Biol. 2005;25:4211-4220.
47. Graham DB, Robertson CM, Bautista J, et al. Neutrophil-mediated oxidative burst and host defense are controlled by a Vav-PLCgamma2 signaling axis in mice. J Clin Invest. 2007;117:3445-3452.
48. Savill J, Hogg N, Ren Y, Haslett C. Thrombospondin cooperates with CD36 and the vitronectin receptor in macrophage recognition of neutrophils undergoing apoptosis. J Clin Invest. 1992;90:1513-1522.
49. Castagna M, Takai Y, Kaibuchi K, Sano K, Kikkawa U, Nishizuka Y. Direct activation of calcium-activated, phospholipid-dependent protein kinase by tumor-promoting phorbol esters. J Biol Chem. 1982;257:7847-7851.
50. Ross GD, Vetvicka V. CR3 (CD11b, CD18): a phagocyte and NK cell membrane receptor with multiple ligand specificities and functions. Clin Exp Immunol. 1993;92:181-184.
51. Ren Y, Stuart L, Lindberg FP, et al. Nonphlogistic clearance of late apoptotic neutrophils by macrophages: efficient phagocytosis independent of beta 2 integrins. J Immunol. 2001;166:4743-4750.
52. Reynolds LE, Conti FJ, Lucas M, et al. Accelerated re-epithelialization in beta3-integrin-deficient mice is associated with enhanced TGF-beta1 signaling. Nat Med. 2005;11:167-174.
53. Colgan J, Rothman P. Manipulation of signaling to control allergic inflammation. Curr Opin Allergy Clin Immunol. 2007;7:51-56.
54. Wynn TA. Cellular and molecular mechanisms of fibrosis. J Pathol. 2008;214:199-210.